



UNIVERSIDADE DE
COIMBRA

João Pedro Olim Castro

**NANOCOMPOSITE HYDROGEL WITH MESOPOROUS
SILICA NANOPARTICLES FOR TISSUE ENGINEERING**

Dissertação no âmbito do Mestrado Integrado em Engenharia Biomédica orientada pela
Doutora Sabine van Rijt e Doutora Benilde Costa e apresentada ao Departamento de
Física da Faculdade de Ciências e Tecnologia da Universidade de Coimbra

Setembro de 2019

This project was developed in collaboration with:

MERLN Institute for Technology-Inspired Regenerative Medicine

Maastricht University



**Maastricht
University**

and

University of Coimbra

1 2 9 0



**UNIVERSIDADE D
COIMBRA**

Esta cópia da tese é fornecida na condição de que quem a consulta reconhece que os direitos de autor são pertença do autor da tese e que nenhuma citação ou informação obtida a partir dela pode ser publicada sem a referência apropriada.

This copy of the thesis has been supplied on condition that anyone who consults it is understood to recognize that its copyright rests with its author and that no quotation from the thesis and no information derived from it may be published without proper acknowledgement.

Acknowledgment

I would firstly like to thank my supervisors, Doctor Sabine van Rijt and Aygül Zengin of MERLN, for the help, guidance, kindness, support and availability to help me at any moment. Thank you for your critics and for pushing me towards the best! And a special thank you for inspiring me to pursue a career in academia!!

To the University of Coimbra, the Faculty of Science and Technology and to Doctor Benilde Costa from the Physics Department, for being there when I needed and help with this project.

I am extremely grateful to my parent that gave me the strength to study, to never give up on me and always believe in me even when I could not, they inspire me to achieve greater things and to fight for my dreams. My sister, that since I am a young boy, became a role model for me and I wish someday I could be like her.

I would like to express my gratitude to my friends, that even with the distance, the true friendship did not go away. To Claudio for contently being there for me, for the best moments and the worst, showing what real friendship is. Joana for the best laughs, Maria for the deep conversations and shows on the airports, Margarida to always slam my head and tries to put some sense in me. Thank you Marta and Mariana for always being there, Sofia for being by my side at every moment and Rute for being the wildest spirit that I know. Joana and Sara for welcoming to this country, for showing me its secrets. Also thank you to the friends that made in Maastricht, and to Ruben for everything.

“Se quiserdes no mundo ser tamanhos,
Despertai já do sono do ócio ignavo,
Que o ânimo de livre faz escravo.”

- Luís de Camões

Abstract:

Introduction: Although hydrogels can be applied in mimicking the native extracellular matrix environment, they generally suffer from weak mechanical properties, which can limit their biomedical application. Mesoporous Silica Nanoparticles (MSN) have been introduced in hydrogels to improve their mechanical properties. Here we investigated MSN as crosslinker agent between PEG chains, to create a hydrogel with desirable mechanical properties to be used in tissue regeneration applications.

Material & Methods: Core and surface functionalized MSNs were synthesized using a sol-gel method. Multi-armed PEG-SH polymer was used to create a hydrogel. The effect of functionalized MSN in the hydrogel was characterized by Rheology to analyze their mechanical properties. Degradation test was carried out by glutathione reductase (GSH). Furthermore, drug release and drug diffusion kinetics were performed to test permeability and release.

Results: Injectable, mechanically strong nanocomposite hydrogel were obtained by using functionalized MSNs as crosslinkers between PEG chains. Effect on the network was found, and possible to see based on the rheology and diffusion assays. On drug delivery rate, the hydrogel encapsulated more drugs, releasing it with some delay compared to hydrogel without MSNs. In addition, this hydrogel showed self-healing capacity and degradability.

Conclusion We demonstrated the modulation on the surface of mesoporous silica nanoparticles and their work as crosslinkers between PEG chains and their changes comparing with PEG hydrogel. Functionalized MSN as crosslinkers in the network, showed improved mechanical properties, while being degradable and self-healing.

Keywords: Nanocomposite hydrogel, Mesoporous Silica Nanoparticles, Functionalization, Dithiol bonds, Mechanical properties.

Resumo:

Introdução: Embora os hidrogéis possam ser aplicados na imitação do ambiente da matriz extracelular, geralmente fornecem fracas propriedades mecânicas, o que pode ser limitante na sua aplicação biomédica. Nanopartículas de sílica Mesoporosas (MSN) têm capturado a atenção em diversos campos de engenharia de tecidos devido a suas características. Aqui, investigamos a utilização de MSNs como agente reticulador entre as cadeias PEG, de modo a criar um hidrogel com propriedades mecânicas desejáveis para uso em aplicações biomédicas e regeneração de tecidos.

Material e Métodos: MSNs funcionalizados no núcleo e na superfície foram sintetizados usando o método sol-gel. Polímero PEG-SH de múltiplos braços foi usado para criar um hidrogel, no qual respectiva caracterização foi realizada. O efeito do MSN funcionalizado no hidrogel foi realizado por testes de reologia de modo a analisar as suas propriedades mecânicas. Devido às ligações ditiol entre MSNs e PEG, teste de degradação foi realizado pela glutatona redutase (GSH). Além disso, a cinética de difusão e fornecimento de fármaco foi realizado para testar a permeabilidade e taxa de distribuição.

Resultados: Nanocomposito Hidrogel mais forte, injetável e *self-healed*, foi obtido usando MSNs com grupos funcionais como reticuladores entre as cadeias de PEG. Através de testes de reologia e difusão, é possível admitir que há efeito na rede do hidrogel. Na taxa de entrega do fármaco, o hidrogel encapsula mais o medicamento, liberando-o com algum atraso em comparação ao hidrogel sem MSNs. Além disso, este hidrogel mostrou capacidade de self-healing e degradabilidade, embora no último, mais testes sejam necessários para uma melhor compreensão.

Conclusão: Demonstramos a modulação na superfície de nanopartículas de sílica mesoporosa e seu trabalho como crosslinkers entre cadeias de PEG e suas alterações em comparação com o hidrogel de PEG. O MSN funcionalizado como reticuladores na rede, mostrou propriedades mecânicas aprimoradas, sendo útil em diferentes aplicações na engenharia de tecidos.

Palavras-chave: Nanocomposito hidrogel, Nanopartículas de sílica Mesoporosa, Funcionalização, Ligações Ditiol, Propriedades mecânicas.

List of content

Acknowledgment	i
Abstract:	v
Resumo:	vii
List of content	ix
List of Tables	xi
List of Figures	xiii
List of Abbreviation	xiv
1 Introduction.....	1
1.2 Application of hydrogels in tissue engineering field	2
1.2.1 Mechanical properties	2
1.2.2 Porosity	3
1.2.3 Injectability	3
1.2.4 Degradation Rate	4
1.2.5 Self-healing	4
1.3 Nanocomposite Hydrogels	4
1.4 Mesoporous Silica Nanoparticles	5
2 Materials and Methods.....	7
2.1 Materials	7
2.2 Synthesis of MSNs.....	7
2.3 Characterization of MSNs.....	8
2.4 Ellman’s Reagent Assay	8
2.5 Hydrogel Formation.....	9
2.6 Rheological Characterization of Hydrogels.....	9
2.7 Diffusion Rate of Hydrogels.....	9
2.8 Drug Release from Hydrogel	9
2.9 Degradation Studies	10
3 Results and Discussion	11
3.1 Synthesis of core-shell functionalized Mesoporous Silica nanoparticles	11
3.2 Quantification of variable functional group densities on MSN surface functional groups.....	12
3.2.1 Ellman’s Reagent	12

3.2.2 ATTO 633 Labelling.....	13
3.3 Hydrogel Formation.....	14
3.3.2 Injectability and Self-healing.....	15
3.3.4 Rheology	16
3.3.5 Degradation Assay	18
3.4 Drug Diffusion and Release.....	21
4 Conclusion	25
5 References:.....	27
Supplementary Information	xxxi

List of Tables

Table 1 - Fluorescent signal intensity of MSNs, which have different functional groups ___12

Table 2 - Concentration of Thiol in the surface of MSNs with normal functionalization___12

Table 3 - Concentration of thiol in the surface of MSNs after modulation _____13

List of Figures

Figure 1-Different type of crosslinking interaction between polymeric chains.....	1
Figure 2 -Representative model of one MSN and its characteristics.....	5
Figure 3 - Mesoporous Silica Nanoparticles (MSN)	11
Figure 4 - Modulation of the functionalization in the surface of MSN-NH ₂ in-SHout.....	13
Figure 5 - Schematic representation of the network bonds of the hydrogel.....	14
Figure 6 - Hydrogel formation.....	15
Figure 7 - Injection of the hydrogel through a syringe with an 18G needle.....	15
Figure 8 - Self-healing assay	16
Figure 9 - Storage modulus (G') and loss modulus (G'') of MSN-PEG hydrogel.....	17
Figure 10 - Rheometer results for strain sweep and self-healing tests.....	17
Figure 11- Storage modulus of three different hydrogels.....	18
Figure 12 - Mechanism of Gluthatione Reductase.....	19
Figure 13 - Degradation Assay by mass loss study.....	19
Figure 14- Degradation of hydrogel in different and higher concentrations of GSH.....	20
Figure 15 - Mass loss study of hydrogels with different MSN functionalization.....	21
Figure 16 – Kinetic Diffusion assay of MSN-PEG hydrogel.....	22
Figure 17 - Drug Release assay from the hydrogel, using PEG hydrogel as a control.....	23
Figure S1 – Calibration curve of Cystein-HCL.....	xxx
Figure S2 - Different solutions of DTNB.....	xxxi
Figure S3 – Hydrogel degradation with 5mM GSH.....	xxxii
Figure S4 - Hydrogel formation with different functionalization of MSN.....	xxxii

List of Abbreviation

APTES	3-Aminopropyl triethoxysilane
CTAC	Cetyltrimethylammonium chloride ^{[1][SEP]}
DLS	Dynamic light scattering ^{[1][SEP]}
DPDS	2,2'-Dipyridyldisulfide
DTNB	5,5'-Dithiobis-(2-Nitrobenzoic Acid)
ECM	Extracellular Matrix
FITC	Fluorescein ^{[1][SEP]}
GSH	Glutathione Reductase
MPTES	3-mercaptopropyl triethylsilane
MSN	Mesoporous Silica Nanoparticle
NHS	N-hydroxysuccinimide esters ^{[1][SEP]}
PBS	Phosphate-buffered saline ^{[1][SEP]}
PEG	Poly(ethylene glycol)
PTES	Triethoxyphensylsilane
SEM	Scanning electron microscopy
TEA	Triethanolamine ^{[1][SEP]}
TEM	Transmission electron microscopy
TEOS	Tetraethyl orthosilicate

1 Introduction

About 30 years ago, the word “biomaterial” started to appear in science fields as a “substance designed for implantation within or incorporation with a living system”, as defined by Joon Bu Park in 1984 [1]. Compared with other types of biomaterials, hydrogels have the advantages of increased biocompatibility, adjustable biodegradability, desired mechanical properties and porous structure [2-4]. Because of this, hydrogels have received increased interest over the past decades in many fields including in tissue engineering, drug delivery, and biosensor fields [2].

A Hydrogel is a three-dimension network consisting of polymeric chains, able to absorb water. This capacity of absorption can go from 10% up to thousands of times of its dry weight, depending on specific properties of the hydrogel, such as the hydrophobicity of the polymer chains and the crosslinking density [3,5]. Their porosity allows hydrogels to be permeable for nutrients, giving them a degree of flexibility similar to natural tissue.

Hydrogels can be prepared from natural or synthetic polymers. Natural polymers show good biocompatibility, although there are some limitations, such as poor resilience, low strength, and possible microbacterial contamination. In contrast, synthetic polymers have well-defined structures that can be modified [6] to improve the mechanical strength and stability [7]. Poly(ethylene glycol) (PEG) is one of the most widely used synthetic hydrogels in medicine. The versatility of the PEG chemistry and its excellent biocompatibility, high hydrophilic nature and drug delivery capacity, make them good candidates for use in tissue engineering applications [8, 9].

Hydrogels are formed by crosslinking hydrophilic polymer chains, which, can be made through physical entanglement and chemical crosslinking. (Figure 1)

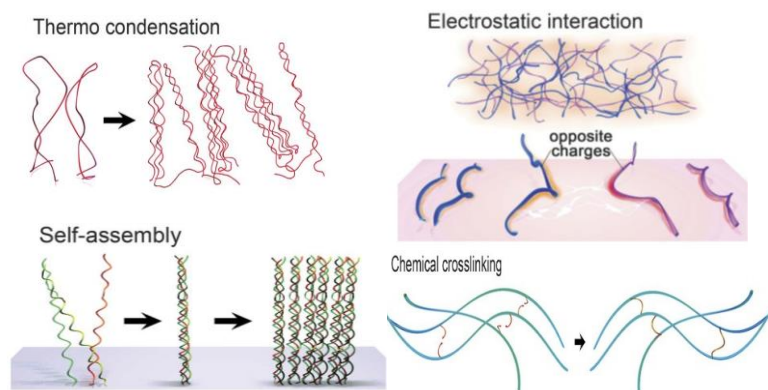


Figure 1- Different type of crosslinking interaction between polymeric chains

Physically crosslinked hydrogels are usually created by intermolecular reversible interactions, such as ionic/electrostatic interaction. The main advantage of this type of crosslinking is the absence of chemical crosslinking agents, which avoids potential cytotoxicity. However, chemical or covalent-crosslinking generally leads to more stable hydrogel structures and higher mechanical properties due to their permanent bonds. This promotes control over properties such as permeability, molecular diffusivity, water content, elasticity, modulus, and degradation rate [10, 11].

One way to create more responsive hydrogels is to use reversible covalent bonds, which gives the advantage of maintaining the covalent crosslinking integrity but also the commutability of physical interaction [10]. Ruiwei Guo and colleagues reported a hydrogel with reversible boronate ester and disulfide bonds. These bonds resulted in a pH, and redox sensitive hydrogel with self-healing properties. [12]

1.2 Application of hydrogels in tissue engineering field

Tissue engineering aims to replace or facilitate the regrowth of damaged or diseased tissue by applying combinations of biomaterials, cells, and bioactive molecules. The main goal of this research area is to restore, maintain, or improve damaged tissues or whole organs in an organism [13].

Extracellular Matrix (ECM) is a network mediated by enzymes during normal and pathological conditions, controlling cell communication and interaction between tissues. Thus, hydrogels in tissue engineering are designed to mimic ECM in order to promote new tissue formation. To do this, several design parameters should be taken in consideration such as its mechanical properties, porosity, injectability, biodegradation, and self-healing, which will be described further. Also, some biological performance parameters, such as biocompatibility and cell adhesion, as well as demonstrating enhanced vascularization are important [13].

1.2.1 Mechanical properties

Hydrogels need to have similar mechanical characteristics as the tissue that it is repairing/substitute, since hydrogel stiffness is known to influence cell behavior. ECM stiffness also takes an important role in both physiological and pathological environment, because it could integrate biomechanical and biochemical properties and support specific

tissue engineering applications [14]. In addition, for harder tissues such as bone or cartilage, hydrogels with a higher mechanical strength are preferred to give load-bearing properties to the materials.

One of the main parameters that control the mechanical properties of hydrogel is the crosslinking density, as reported by Bryant SJ et al, whereas, changing the crosslinking density of a PEG-based hydrogel, influences the cell growth and their morphology [9,10]. However, many efforts have been focused on increasing the mechanical strength of hydrogels, for example using double network systems. Recently, nanocomposites; the introduction of nanoparticles in the hydrogels has been shown to increase the mechanical strength [15].

For example, Wang, Q. et al, developed a strong hydrogel by making tight rigid crosslinked hydrogels with a double network, increasing the mechanical properties and Young's modulus. Incorporation of silica nanoparticles in the hydrogel resulted in an increase in the young's modulus by an order of magnitude. Such increase in toughness was attributed to the combined effect of silica/polymer hydrogen bonding [16].

1.2.2 Porosity

The porosity plays an important role in directing tissue regeneration. It allows a homogeneous cell distribution and interconnection between the tissues. After implantation, the porosity of the hydrogels affects the rate of angiogenesis, which is important for regenerating tissues as vascularization has a significant role in cell survival, migration and proliferation.

Manipulation of the porous size of a hydrogel can influence the outcome of the cells; porous diameters between 5-15 μ m were optimized for fibroblast ingrowth, whereas for 100-350 μ m was shown to be better for bone regeneration [17].

1.2.3 Injectability

Usually biomaterials are developed outside of the organism and are implanted by surgical intervention. In order to reduce the invasiveness, injectable hydrogels afford a solution to that problem. For a hydrogel to be injectable, it has to have some specific characteristics e.g. the gel should be in a solution before being injectable, and should directly form after injecting or have shear-thinning properties [18].

1.2.4 Degradation Rate

Controllable biodegradability is an important characteristic for hydrogels applied in the field of tissue engineering, because it allows the hydrogel to be replaced by new growing tissue.

Degradation of a hydrogel can be possible through several mechanisms such as hydrolytic or enzymatic pathways. A promising approach of a controlled degradation is to incorporate enzymatically cleavable sites. One possible example is the Glutathione reductase for the cleavage of di-thiol bonds. Aaron D. Baldwin et al, prepared a hydrogel with maleimide-functionalized low molecular weight heparin (LMWH) crosslinked with a multi-arm thiol-functionalized PEG, in which they manage to degrade the hydrogel, by reduction of disulfide bonds using glutathione (GSH) [19].

Moreover, degradation of the hydrogel can lead to control over growth factor or drug delivery in order to improve stem cell differentiation, proliferation, or for wound healing [14, 20].

1.2.5 Self-healing

Self-healing is an outstanding property of tissues like bone or skin; therefore, hydrogels with self-healing properties would be of interest in the field of tissue engineering.

Self-healing of hydrogels are characterized by the regaining of their mechanical strength after its molecular interactions are being broken [2]. Wen Jing Yang et al, reported a self-healing antifouling and antibacterial hydrogel that can be used as a coating for long-term biomedical applications. This hydrogel was made with two functionalized monomers and a disulfide-containing crosslinker, that due to the disulfide exchange reaction, obtained self-healing properties [21].

In another example, Bastings, M. M. C et al, created an injectable pH-switchable supramolecular hydrogel for myocardial infarctions. The hydrogel-solution is loaded with growth factors, and upon contact with tissue gelled, reducing the infarcted scar [22].

1.3 Nanocomposite Hydrogels

Nanocomposite hydrogels are interesting hybrid materials that can overcome some limitations regarding traditional hydrogels, such as improved mechanical properties and increased functionalities like, additional optical, and swelling properties [23]. These hydrogels also show good compatibility for cell adhesion and proliferation [23]. For example,

Wishulada Injumba et al. prepared PEGylated silica-iron oxide nanocomposite as drug carriers to modulate cell cytotoxicity and inflammatory responses. [24].

Some nanocomposite hydrogels have shown to obtain highly elastomeric behaviour, improved mechanical strength and better physiological stability compared to hydrogels without nanoparticles. Gaharwar et al. were able to form an injectable nanocomposite hydrogel with silica nanoparticles and poly (ethylene glycol) (PEG) and resulted in a nanocomposite hydrogel with enhanced mechanical properties and cell adhesion, which can be used as filler in orthopedic applications. [25]

One way to improve the bioactivity of hydrogels is by using inorganic ceramic nanoparticles supplemented polymers. These inorganic nanoparticles consist of minerals that are present in the living organism. For example, Silicon is present in most of the ceramic nanoparticles and plays a role in osteogenic differentiation in stem cells and promotes collagen synthesis [26]. Thus, introducing these particles in hydrogels, is possible to add additional bioactivity characteristics to the polymeric network.

1.4 Mesoporous Silica Nanoparticles

Silica-based nanomaterials have received enormous attention in the fields of biocatalysis, bio-optics and drug delivery. Silica is highly biocompatible and silica-based nanoparticles have already been approved for human clinical trials [27].

Mesoporous Silica Nanoparticles (MSNs) are silica-based nanoparticles relatively new to the field of regenerative medicine and tissue engineering. This new material has shown extraordinary results due to their large surface area and pore volume, allowing them with high loading capacity, ideal for drug delivery and protein adsorption for cell adhesion and proliferation (Figure 2) [28, 29]. Furthermore, their surface chemistry can be easily modified. This characteristic allows functionalization of the internal and external surface. Surface chemistry on the other hand, can be employed to modulate surface reactivity, which also influences cell material interactions [30]. Also, their tunable size can facilitate the endocytosis in living organisms without any significant cytotoxicity. [31]

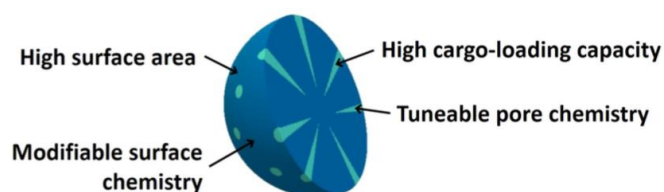


Figure 2 - Representative model of one MSN and its characteristics

The high drug loading degree of MSNs may offer a solution to avoid the burst release of drugs that is normally observed. Zhaofu Zhang, Shuo Wang et al, design a hydrogel using MSNs as physical crosslinkers between poly(*N*-isopropylacrylamide) (PNIPA) chains. Due to drug loading capacity of the MSN and the blood biocompatibility of PNIPA, the nanocomposite hydrogels had great potential in drug transport and temperature-activated drug release [32].

Based on the properties described about the MSNs, Wang, N et al, noticed that when introduced this kind of silica-nanoparticles in a gelatin methacryloyl, the mechanical properties can be tuned. With the addition of different concentrations of MSN-COOH (MSN with Carboxylic acid functionalization), hydrogels with different pore sizes and mechanical properties were obtained. The MSNs worked as a filler in the hydrogel changing it's properties, promoting viability and adhesion of stem cells [33].

Another group of scientist, shown that interactions between inorganic hybrid crosslinker and polymer chains, enable a hydrogel with improved mechanical properties. This study shows that silica-nanoparticles increased, in a significant way, the stiffness of the hydrogel [34]. Based on this results, studies have been made whereas inorganic nanoparticles have been introduced as crosslinkers between the polymer chains in the hydrogel, increasing their mechanical properties: tensile and compreenhise strengh [35].

The present study aims to investigate whether thiol functionalized mesoporous silica nanoparticles (MSN) can form reversible covalent interations with functionalized multi-arm PEG-Thiol to form an injectable, self-healing nanocomposite hydrogel. This way, certain mechanical characteristics can be tuned, degradation ratio can be controlled and loading drug capability be studied, making this hydrogel interesting for tissue engineering applications.

2 Materials and Methods

2.1 Materials

Tri-ethanolamine (TEA), Tetraethyl orthosilicate (TEOS), 3-Aminopropyl triethoxysilane (APTES), Triethoxyphenylsilane (PTES), 3-mercaptopropyl triethylsilane (MPTES), Cetyltrimethylammonium chloride (CTAC), absolute ethanol, hydrochloric acid (HCl, 37%), ammonium nitrate (NH_4NO_3), 5/6-carboxyfluorescein succinimidyl ester (NHS-FITC) and ATTO 633-maleimide. 2,2'-Dipyridyldisulfide (DPDS), 4arm-PEG20K-SH, 5,5'-Dithiobis-(2-Nitrobenzoic Acid) (DTNB) and Glutathione Reductase (GSH). All chemicals were purchased from Sigma Aldrich GmbH (Germany) Absolute ethanol was purchased from VWR (US).

2.2 Synthesis of MSNs

MSNs with amine functional groups in the core and thiol functional groups on the surface were synthesized as described in literature [36]. Briefly, a mixture of TEA (14,3g ,95,6 mmol) , TEOS (1,466g, 7,37 mmol), PTES (110,8 mg ,0,461 mmol) and APTES (82,65mg , 0,461 mmol) was heated at 90°C for 20 minutes without stirring (Solution 1). A solution of CTAC (2,41mL; 7,29 mmol) and Milli Q-water (21,7g H_2O) (Solution 2) was heated at 60°C with stirring for 20min. Solution 2 was rapidly added to solution 1, and the mixture was left stirring (700rpm) for 20 minutes while cooling down to room temperature. Afterwards, TEOS (138.2 mg; 0,922 mmol) was added to previous solution mixture in four equal increments (37 μL /34.55 mg each) every three minutes and mixture was left stirring for another 30 min at room temperature. Subsequently TEOS (19,3mg; 92,5 μmol) and MPTES (20,5mg; 92,5 μmol) was added to the mixture and left it overnight stirring at room temperature.

The next day, 100mL of absolute ethanol was added, the MSN were collected by centrifugation, Centrifuge 5430R, (7830 rpm for 20min) and redispersed it in absolute ethanol. For template extraction, MSNs were redispersed in 100mL ethanol solution containing 2g of NH_4NO_3 . The solution was under reflux (90°C, oil bath temperature) for 45min. The MSNs were collected by centrifugation after extraction and washed with absolute ethanol, previously of being extracted under reflux for 45min in a solution of 90mL of Absolute Ethanol and 10mL of HCl. Afterward, the nanoparticles were collected by centrifugation and washed two more times with absolute ethanol before being stored at -20°C.

2.3 Characterization of MSNs

Size and zeta potential of MSNs were analyzed by Malvern Zetasizer Nano. For this analysis, particles were suspended in absolute ethanol at a concentration of 0,5mg/mL. For SEM imaging (acquired in Chemelot Campus), samples of 0,5mg/mL were sputtered with a 4 nm layer of iridium coating. To confirm the chemical groups of the core and of the surface, MSNs were labelled with fluorescent dyes in order to confirm the successful functionalization. 5/6-carboxyfluorescein succinimidyl ester (NHS-FITC) and ATTO 633-maleimide were used to label the amine groups in the core and the thiol groups on the surface, respectively. For FITC labelling, 20 μ L of the dye solution (6,3mg/mL in absolute ethanol) was used per 1mg of MSN. Per reaction, 0,5 μ L of ATTO solution (5mg/mL in DMF) was used per 1mg of MSN. Coupling reactions of the dyes with MSNs were always performed in 1 mL absolute ethanol. Briefly, MSNs were suspended in absolute ethanol and the dye solution was added. The mixture was left for overnight stirring in the dark at room temperature, and on the next day, the MSNs were collected by centrifugation (14 000 rpm for 20 min) and washed three times with absolute ethanol. MSNs were resuspended in absolute ethanol at a concentration of 10 mg/mL and fluorescent measurements were performed using microplate reader (CLARIOstar BMG LABTECH). The fluorescent for FITC labelling is detected at λ_{exc} =488-14nm and λ_{emi} =535-30nm and for ATTO at λ_{exc} =620-30nm and λ_{emi} =680-40nm.

2.4 Ellman's Reagent Assay

Ellman's reagent protocol was used to determine the concentration of thiol functional groups on the surface of the MSNs [37]. Firstly, freeze-dried nanoparticles (0.3 mg/ml) were dispersed in sodium phosphate buffer (pH 8; 0,5M) and left to incubate (37°C, 500rpm) for 1h prior the assay. Afterwards, 500 μ L of MSN solution was mixed with 500ul of DTNB solution (0,3 mg/mL in sodium phosphate buffer) and the sample were left to incubate (37°C, 500rpm) for 3h. Absorbance was measured by microplate reader at 420nm.

Parallel to this assay, a calibration curve with cysteine-HCl was performed to establish a way between the quantification of thiol and the absorbance. Cysteine-HCl concentrations used were between 10 and 520 μ mol, the samples were prepared the same way that the protocol described above.

2.5 Hydrogel Formation

Hydrogel formation was obtained through the mixture of freeze dried MSN and 4-armPEG-SH in PBS (2,67wt% and 13,3wt%, respectively) in presence of 2,2'-Dipyridyldisulfide (DPDS, 8 μ M in PBS-ethanol solution) in a 75%-25% ratio. The solution was homogenized and left it for incubation at room temperature for half an hour.

2.6 Rheological Characterization of Hydrogels

Rheological measurements were performed Discovery HR-2 machine, whereas the late time cure was monitored by measuring the storage and loss modulus, G' and G'' , respectively using a cone plate 20mm. The test methods employed were oscillatory time sweep, frequency sweep and strain sweep. During time sweep test, ω , frequency and strain were maintained for 20 min (1Hz and 1% respectively). Strain sweep test, constant frequency was used (1Hz) and strain values increased from 0,1 to 1000. In frequency sweep test, strain value was kept constant at 1% and frequency values changed from 0,1 to 10Hz.

All experiments were made with 80 μ L hydrogel (2wt% MSN) and mechanical strength and self-healing tests were performed by Aygül Zengins.

2.7 Diffusion Rate of Hydrogels

To test the diffusion of the hydrogel, Rhodamine B was used. This diffusion behavior was measured by fluorometer (λ_{exc} =553nm and λ_{emi} =627nm) during 42h at low stirring rate.

MSN-PEG and PEG hydrogels (each volume 150 μ L) were made on top of membrane for disposable cuvettes (Slide-A-Lyzer) and left for swelling during 24h submersed in 150 μ L PBS. Afterward, the remaining PBS was removed, cuvettes were filled with PBS (3,2mL) and the membranes with hydrogel were inserted. Subsequently the 150 μ L of Rhodamine B solution (70 μ M) was added to the top of the hydrogels and fluorescent intensity was recorded.

2.8 Drug Release from Hydrogel

Rhodamine B was used as a model drug to study of release behavior of these hydrogels. Rhodamine B (4mM) was mixed in the DPDS solution. When DPDS was added to the MSN-PEG mixture, the hydrogel formation occurred with Rhodamine B.

The swelling and measurement step was identical as described in 2.7, although 150 μ L of PBS was added on top instead of the probe inside of the fluorometer.

2.9 Degradation Studies

Hydrogel samples were prepared on Eppendorf tubes and left for 24h to incubate at 37°C in static conditions in Phosphate-Buffered Saline (PBS) to achieve equilibrium swelling. The remaining PBS buffer was removed and weight the initial weight of the swelled hydrogel. The hydrogels were immersed in a Glutathione (GHS) solution of different concentrations (mentioned in the next Chapter) and a control group only immersed in PBS. At predetermined time points, the excess solution was removed and the mass of the hydrogel was measured. The percentage of mass remaining was calculated as:

$$\frac{[(\text{Raw mass}) - (\text{Mass of Eppendorf})] - (\text{Swelled mass})}{[\text{Swelled mass}]} * 100 \quad (1)$$

3 Results and Discussion

3.1 Synthesis of core-shell functionalized Mesoporous Silica nanoparticles

Mesoporous silica nanoparticles with amine functional groups in the core and thiol functional groups on the surface (MSN-NH_{2in}-SH_{out}) were successfully synthesized using a delayed co-condensation protocol, as described previously [36]. DLS and Zeta potential results showed that MSNs are positively charged (+55mV) and have homogeneous size distribution (around 200 nm) with a polydispersity index (PdI) value of 0.18 (Figure 3).

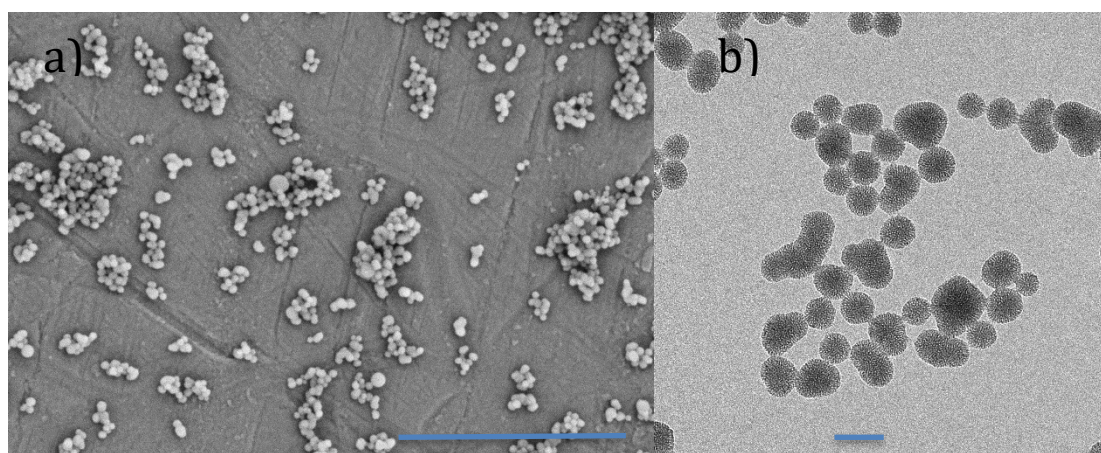


Figure 3 – Mesoporous Silica Nanoparticles (MSN)

MSNs with amine functionalization on the core and thiol functionalization on the surface. a) Image with SEM technique (scale bar = 2 μ m); b) Visualization with TEM (scale bar = 100nm). (SEM image taken by Aygül Zengins and TEM images takes by Chloe Trayford)

In order to confirm successful core-shell functionalization, chemical functional groups were labeled with fluorescent dyes. The particles were first loaded with fluorescein (FITC-NHS). In here, the amine groups on the MSN surface react with the N-hydroxysuccinimide ester (NHS) groups and give a fluorescent signal, which was later read in the Microplate-reader. Afterward, the same particles were loaded with ATTO 633-Maleimide. This dye has maleimide, which will bond to the free thiol groups present in the surface of the nanoparticles.

As a control, non-functionalized MSNs (MSN-OH) were stained with these fluorescent dyes. The results (Table 1) showed that the fluorescent signal of MSN-OH was similar to ethanol, while the MSN-NH_{2in}-SH_{out} has a strong fluorescent signal.

Table 1 – Fluorescent signal intensity of MSNs, which have different functional groups

	MSN-NH _{2in} -SH _{out}	MSN-OH
FITC	226623	35
ATTO 633	200623	24

3.2 Quantification of variable functional group densities on MSN surface functional groups

After proving the functionalization of the nanoparticles, the next step was to try to modulate functionalization, by decreasing the ratio of MPTES (Thiol groups) on the surface. This modulation would influence the behavior on the crosslinking network, possibly changing mechanical properties and degradation rate of the hydrogel.

In order to analyze the surface modulation, two assays were done, Ellman's Reagent and ATTO 633 labelling.

3.2.1 Ellman's Reagent

DTNB reacts with a free sulfhydryl group (R-S-) resulting in a colored species 2-nitro-5-thiobenzoic acid (TNB) that can be measured with a Microplate reader.

Firstly, a calibration curve was prepared with different concentrations of cysteine-HCl. (Figure S1). MSN-NH_{2in}-SH_{out} were labeled like described previously and the results are shown in Table 2.

Table 2- Concentration of Thiol in the surface of MSNs with normal functionalization

The concentration of Thiol in MSN-NH_{2in}-SH_{out} batches	
MSN-SH	20,77 μ M
MSN-NH ₂ -SH (9mg/ml batch)	21,96 μ M
MSN-NH ₂ -SH (12mg/ml batch)	20,69 μ M

As possible to observe, the concentration of thiol seems approximately the same, although with some changes between the batches. These results show that the assay works

and it is possible to determine the concentration on the surface of the nanoparticles.

Hereinafter, the next step is to try to modulate the surface, reducing the MPTES concentration to 25%, 5%, 1% and 0.1%, being designated MSN-25%, MSN-5%, MSN-1% and MSN-0.1% respectively.

On the MSN-5%, MSN-1% and MSN-0.1%, this assay was performed and the concentration of thiol on the surface was determinate, being shown in Table 3.

Table 3 – Concentration of thiol in the surface of MSNs after modulation

The concentration of thiol in the previous batches	
MSN-NH ₂ -SH (100%)	30,5 μM
MSN-NH ₂ -SH (5%)	26,4 μM
MSN-NH ₂ -SH (1%)	25,0 μM
MSN-NH ₂ -SH (0.1%)	24,9 μM

Based on results shown previously, there is no difference in the concentration of thiol groups on the surface of the MSN-NH₂_{in}-SH_{out}. With this is possible to presume that either the functionalization is lower than the 100% according to synthesis protocol, and/or, the Ellman's Reagent has a minimum sensitivity, which is not possible to detect (Figure S2). To ensure these possibilities, ATTO 633 labelling was performed.

3.2.2 ATTO 633 Labelling

To understand the modulation, ATTO 633 labelling was performed. As described before, this dye has maleimide that bonds to the free SH groups, giving a fluorescent signal that can be read by Microplate-reader. Each percentage on the graph corresponds to the functionalization of thiol in the surface of nanoparticles, according to synthesis.

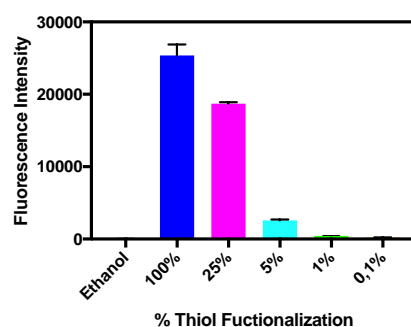


Figure 4 - Modulation of the functionalization in the surface of MSN-NH₂_{in}-SH_{out}
Each percentage corresponds to the functionalization of thiol in the surface of nanoparticles, according to synthesis

Based on the results shown in Figure 4, it is possible to conclude that there is a significant difference in signal between MSN-NH₂-SH (100%) and MSN-NH₂-SH (0.1%). This result exhibit that the modulation of the surface functionalization of the nanoparticles was successfully achieved.

3.3 Hydrogel Formation

Moving towards the formation of the hydrogel, 4-arm PEG-SH was used as the polymer chain, while MSN-NH_{2in}-SH_{out} worked as crosslinkers. In order to achieve this formation, DPDS was used as an initiator because of the S-S group. Due to the presence of free thiol groups in the surface of MSNs and the arms of PEG, these would compete for this bond this making dithiol bridges between the chains and the nanoparticles by reversible covalent interactions in order to be in a more stable state. (Figure 5)

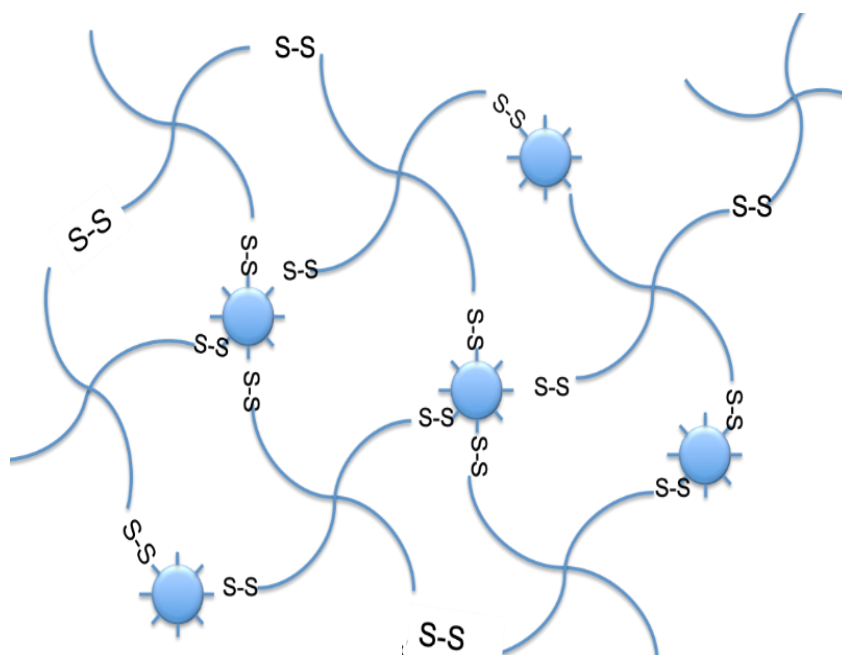


Figure 5 - Schematic representation of the network bonds of the hydrogel

The functionalization on the surface of the MSNs makes it able to bond to multiple chains of 4arm-PEG-SH, creating a more crosslinked network.

MSN-NH_{2in}-SH_{out} was mixed with 4arm-PEG-SH in PBS and then, solution of initiator was added to this mix. After 20min, the hydrogel was formed (Figure 6).

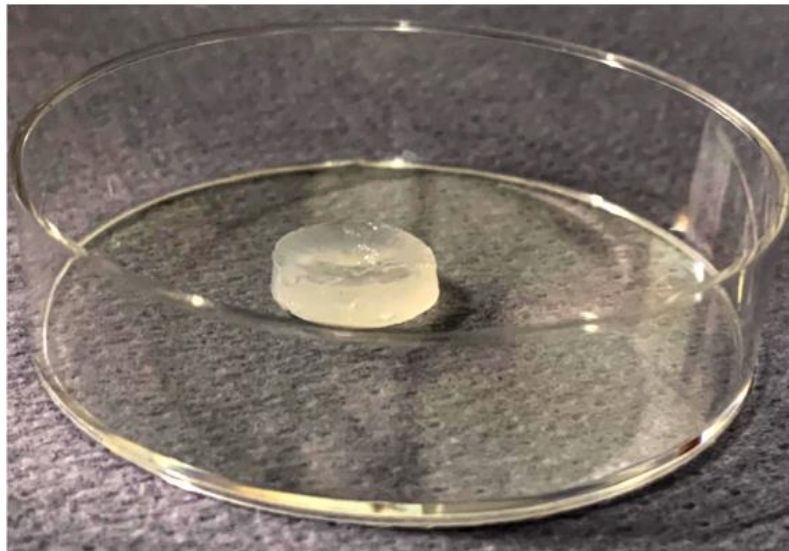


Figure 6 - Hydrogel formation

This shows that it is possible to achieve a hydrogel formation whereas the MSN is part of the network.

3.3.2 Injectability and Self-healing

A good and beneficial characteristic of hydrogels is their injectability. This makes them useful in medical fields without the need for invasive surgery. Therefore, after the hydrogel is formed, it was put in a syringe with an 18G needle to evaluate this property.

The hydrogel was dyed with red food dye to help visualize the injectability capacity as shown in Figure 7.

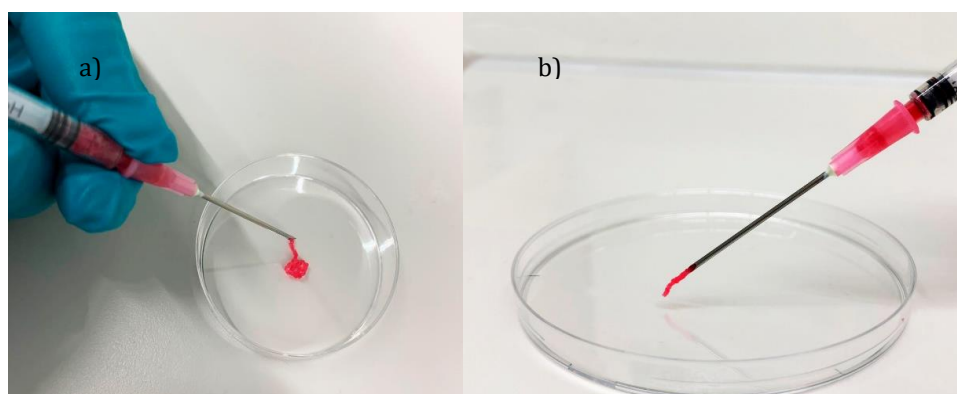


Figure 7 - Injection of the hydrogel through a syringe with an 18G needle

The hydrogel was dyed with a red food dye to help in the visualization of the injectability. a) View from a top, being used as filler; b) injecting the hydrogel.

Due to disulphide exchange reactions, this hydrogel has capacity to reform the broken bonds, as described in previous studies. So, two hydrogels were cut in half and each half put back together. Afterward, a few drops of DPDS solution were added in the interface between the gels and after 4h incubation, the hydrogel restored its behaviour as only one hydrogel (Figure 8).

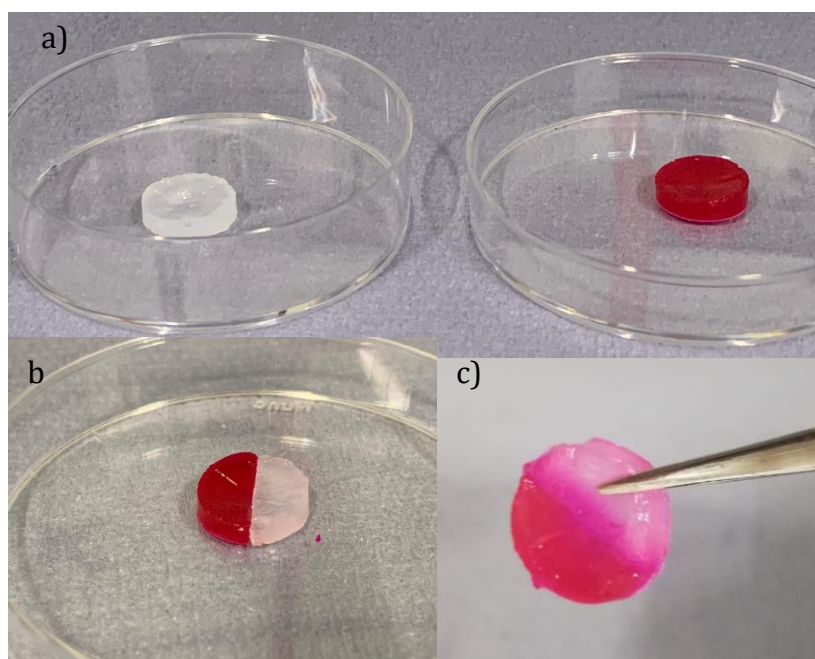


Figure 8 - Self-healing assay

a) Two MSN-PEG hydrogels. The one on the right was added Rhodamine B to make this red colour. b) The hydrogels were cut and each half was put in contact. c) The hydrogel self-healed.

3.3.4 Rheology

The mechanical behavior of the hydrogels was analyzed by rheology. Hydrogels are formed spontaneously and reach a stable plateau value in 20 minutes, maintaining a linear viscoelastic region (frequency of 1 Hz and a strain of 1%) (Figure 9). In here, it is possible to see the mechanical behavior of the MSN-PEG hydrogel, whereas started around 1200Pa, reaching 10kPa. During the course of the reaction, both G' and G'' increase, and G' becomes greater than G'' once gelation occurs

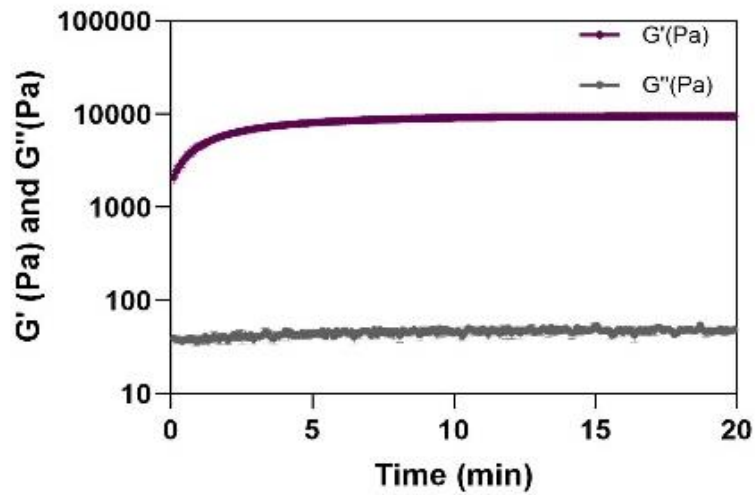


Figure 9 - Storage modulus (G') and loss modulus (G'') of MSN-PEG hydrogel

To test self-healing mechanics, strain sweep measurement was used to see at which strain the hydrogel breaks. (Figure 10)

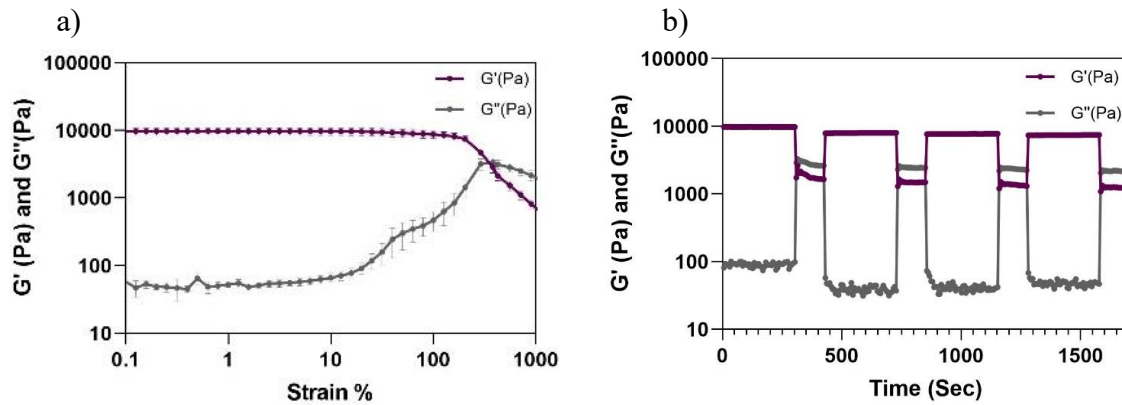


Figure 10 - Rheometer results for strain sweep and self-healing tests
 a) Strain sweep test; b) Self-healing of the hydrogel

The strain sweep test shows that with a 380% strain, the hydrogel breaks its networks. This is proved by the increased of the loss modulus (G'') and the decreases of the storage modulus (G'). Based on this result, self-healing test was made whereas strain between 500% and 1% with a frequency of 1 Hz exhibit a rapid self-healing property, supporting the macroscopic test described previously.

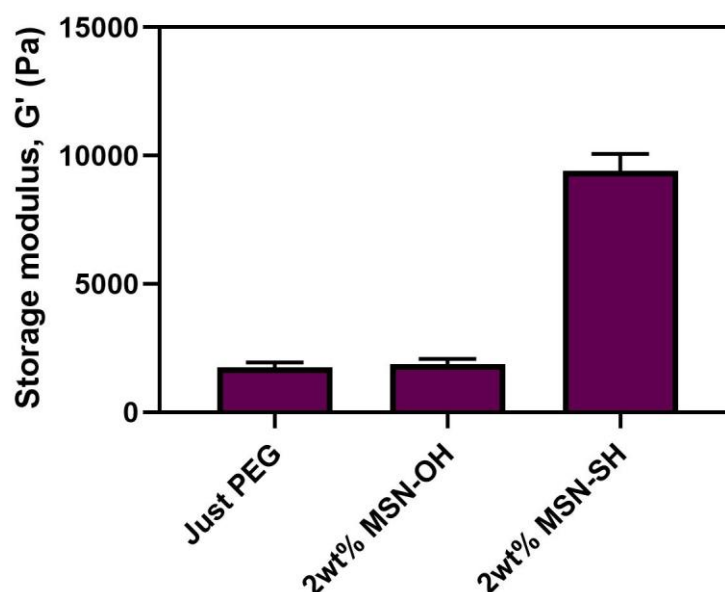


Figure 11 - Storage modulus of three different hydrogels.
PEG-hydrogel, MSN-OH+PEG hydrogel and MSN-NH_{2in}-SH_{out} +PEG hydrogel

By analysis of Figure 11, the storage modulus of 2wt% MSN-OH shows no significant difference between PEG hydrogel, meaning that MSN-OH works as a filler in the network. However, when functionalization is done, MSN-NH_{2in}-SH_{out} increases substantially the properties (2wt%). This evidence means that MSNs with functionalization work as crosslinkers between the chains, increasing the crosslinking density and therefor the mechanical properties, and not as fillers like previous studies has shown.

3.3.5 Degradation Assay

After testing the mechanical properties of the hydrogel, degradation behaviours of the hydrogels were studied in glutathione containing the environment. Glutathione plays a key role in maintaining proper function and preventing oxidative stress in human cells. Glutathione reductase (GSH) is a redox agent that mediates the formation and degradation of

behaviour bridges (Figure 12). The concentration of intracellular glutathione is between 1 and 10mM [38]. While extracellular glutathione concentration is between 1-20 μ M [39].

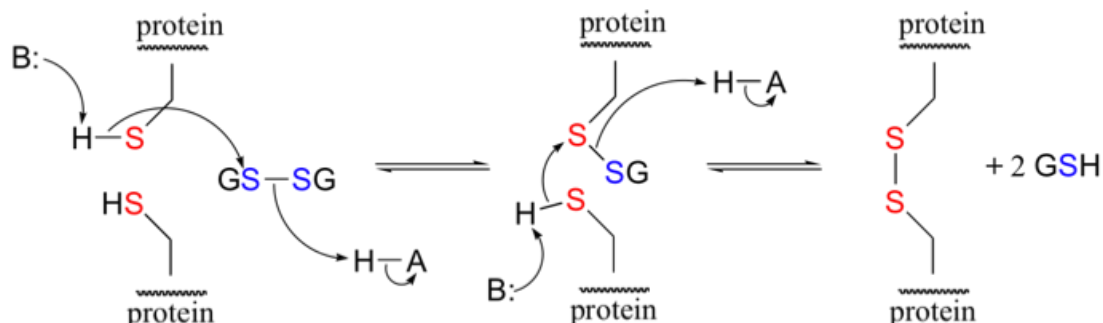


Figure 12 - Mechanism of Glutathione Reductase (Adapted figure [40])

In order to observe the degradation behavior, mass loss method was used. To do that, hydrogels were prepared in triplicates and incubated in three different GSH concentration (2 μ M, 10 μ M, 20 μ M) and Phosphate-Buffered Saline (PBS) solution as a control. The mass of hydrogels in the Eppendorf tube was measured, in order to create a degradation ratio based on the swelling capacity. For the first 24hs, the GSH solution was changed and after, approximately, one week, the time points were prolonged for twice a week, an later for once a week. Obtaining the results shown in the next Figure 13.

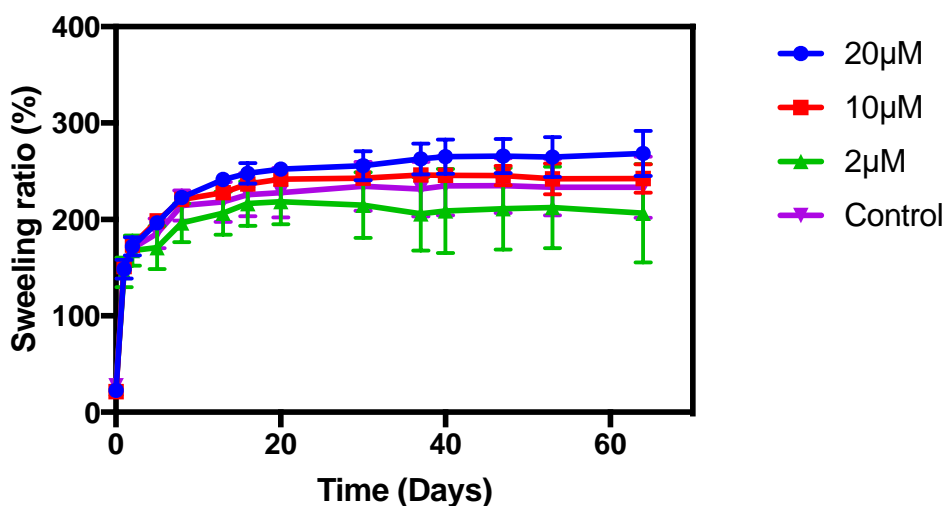


Figure 13 - Degradation Assay by mass loss study

Hydrogels were immersed in different concentrations of GSH according to physiological conditions.

GSH attacks to the behaviour (S-S) bonds between PEG-PEG and MSN-PEG and causes degradation of hydrogels. From the figure 13, it can be seen that hydrogels swelled during the incubation in PBS and glutathione containing environment. This swelling behaviour is expected due to the porous nature of hydrogels. However, there was no degradation during incubation. Therefore, a new study was performed, whereas the GSH concentration was equivalent to the intracellular GSH values in order to understand if the hydrogels can degrade in a shorter time period.

After 24 hours incubation in the GSH solution (5mM), the hydrogels were completely degraded. (Figure S3)

In order to find the best glutathione concentration to observe degradation behaviour of the hydrogels, varying concentrations of GSH (100 μ M, 300 μ M and 500 μ M) were used. To mimic the dynamic environment of ECM, hydrogels were shaking at 300rpm (Figure 14)

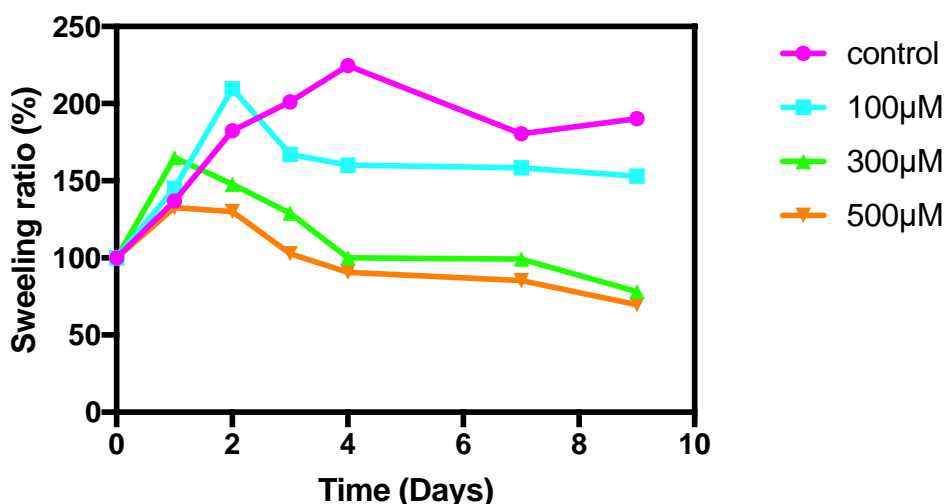


Figure 14 - Degradation of hydrogel in different and higher concentrations of GSH

The hydrogel only with PBS, the control, is in a continuous swelling state, whereas the others are degrading in every time point, this gives a general idea on which GSH to use for further assay.

The results show that hydrogels incubated in 300 μ M and 500 μ M GSH are degraded in a similar trend. The 300 μ M GSH concentration was chosen for the next degradation studies.

In order to modulate the degradation behaviour of hydrogels, MSNs were synthesized varying thiol groups on the surface and different hydrogels were made, with MSNs with different functionalization on the surface (Figure 15). It is to expect, due to less thiol bonds

on the surface of the nanoparticles, the degradation would occur at a faster rate. The next graph shows the different hydrogels with the different MSN's ratios of thiols.

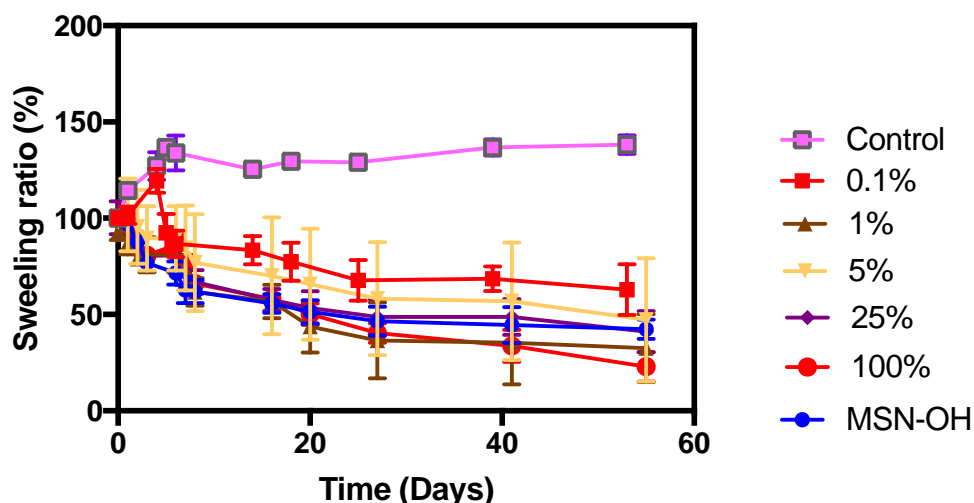


Figure 15 - Mass loss study of hydrogels with different MSN functionalization
 The control was MSN with normal functionalization, and the different percentages are referred to the degree of functionalization as described before. MSN-OH is the hydrogel with MSNs with no functionalization of the surface

Owing to some errors, two groups had to be done from the beginning, being with 48h delay from the others, as it is possible to see for Control and 0.1%.

There is some difference in the degradation rate between the different hydrogels, although it is not what we were expecting. This means that with a lower concentration of thiol on the nanoparticles, the network bonds still remain. One possible explanation for these results is that, with the lack of MSN-PEG bonds, PEG may form more bonds with itself. This means, basically, that is very hard to modify the network of the hydrogel with only this mechanism. More studies need to be done in order to understand how much thiol bonds there is in the network between PEG-MSN.

3.4 Drug Diffusion and Release

As reported in the literature, most of these types of hydrogels are used in drug delivery system. Therefore a study of how this hydrogel diffuses and the release of a drug is necessary.

One hydrogel was immersed in Rhodamine B solution in order to test its permeability and another one was loaded with Rhodamine B in the network, to understand its behaviour. In both cases, only PEG hydrogel was used as a control (Figure 16).

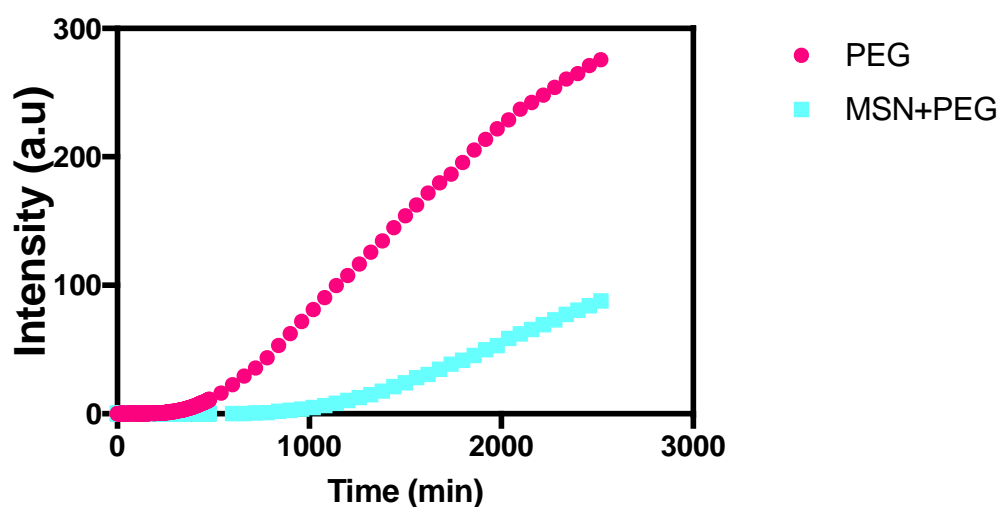


Figure 16 - Kinetic Diffusion assay of MSN-PEG hydrogel using PEG hydrogel as a control
 The cuvette had a membrane with hydrogel and Rhodamine B solution of top, which, through out the time, the Rhodamine B passes through the hydrogel and the membrane to the cuvette, being read by the Fluorometer. This assay was left over 42h

In this diffusion assay, it is possible to observe that the PEG hydrogel shows a better permeability than the MSN-PEG hydrogel. This means, according to literature, that MSN-PEG hydrogel is more crosslinked than PEG [41]. One possible explanation that for the intensity is not the same at the end of the assay, may be due to Rhodamine B be entrapped in the porosity of the MSNs. One possible way to understand that mechanism is to use some small beads, around 20nm. These beads will not interact with the MSNs and will give a more reliable result.

Moving towards the drug release, MSN-PEG hydrogel takes longer to release the same amount of Rhodamine B than PEG hydrogel. This could be useful in longer treatments where a drug should be released later into the environment, avoiding a burst release that is usually observed (Figure 17).

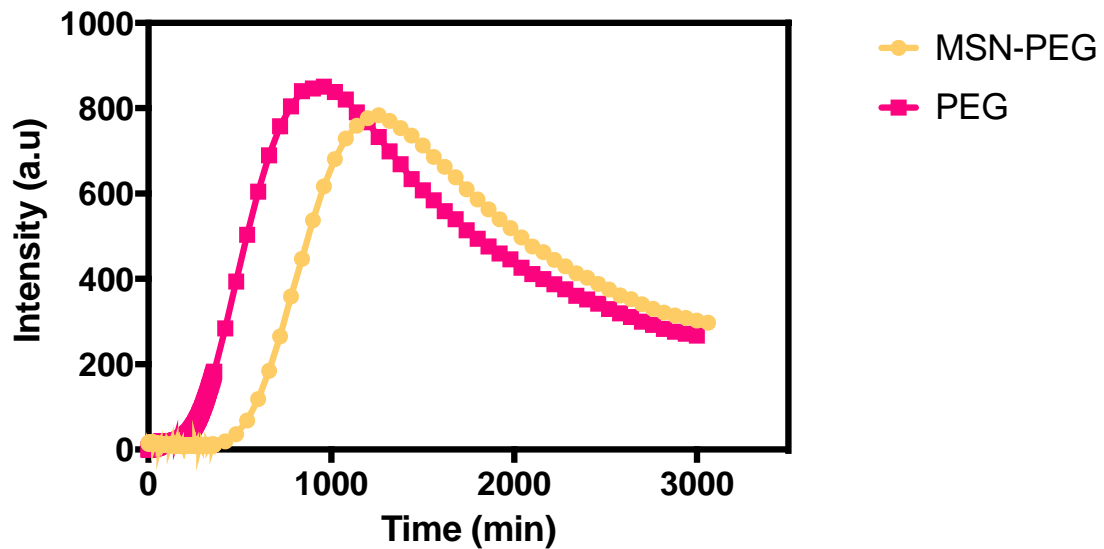


Figure 17 - Drug Release assay from the hydrogel, using PEG hydrogel as a control.

The cuvette had a membrane with hydrogel with Rhodamine B in the network, which, through out the time, the Rhodamine B is released from the hydrogel, being read by the fluorometer. This assay was left over 50h

Although these promising results about this hydrogel, some more assays should be done. For example, toxicity assays in vitro, or different drugs with different molecular weights and sizes should be tested for diffusion and release. Because different treatments may require different methods of drug release and, another assay, is the degradation, but in vitro in the certain physiological conditions, where it would be possible to see some real degradation of the hydrogel

4 Conclusion

Nanocomposite hydrogels have been capturing enormous interest in tissue engineering applications due to their increased properties such as, improving mechanical properties or creating good cell environment. In particular, MSNs are interesting in these nanocomposite networks because of their properties, such as drug-loading capacity, easy surface modification and biocompatibility. In this work, we showed that mesoporous silica nanoparticles with core and surface functionalizations are possible to obtain within uniformity in shape and pores structure.

Due to thiol functionalization on the surface, MSNs are used as crosslinkers, obtaining strong self-healing, injectable, hydrogels. Based on results shown before, these hydrogels have more crosslinking density, reducing their permeability, but increasing their drug release. This property could be very useful for a long-term drug release instead of a burst release.

Moreover, when functionalized MSN work as crosslinker agent, mechanical properties increase significantly when compared to MSN-OH PEG hydrogels and PEG hydrogels.

In addition, these hydrogels present self-healing capacity very useful for tissue regeneration, although their degradation is not completely understood. The presence of GSH degrades the dithiol bonds, however, this behaviour is observed in higher concentrations of this agent. Thus *in vitro* assays need to be done for a better perceptive.

In conclusion, MSNs are a multi-functional tool used in diverse areas of tissue engineering because of its innumerable advantages. By modifying their surface, these nanoparticles can work as crosslinkers between 4arm-PEG-SH chains in a hydrogel, increasing substantially the mechanical properties of this hydrogel, later to be used in biomedical application. Although, some tests about toxicity need to be done in order to understand cell behavior with this type of nanocomposite hydrogel before being used in biomedical field

5 References:

- [1]. Park, J. B. (1984). *Biomaterials Science and Engineering*. Springer US.
- [2]. Zhang, Y. S., & Khademhosseini, A. (2017). Advances in engineering hydrogels. *Science*, 356(6337). <https://doi.org/10.1126/science.aaf3627>
- [3]. Allan S. Hoffman. (2012). Hydrogels for biomedical applications. *Advanced Drug Delivery Reviews*, 54, 1, 1 2002. <https://doi.org/10.1016/j.addr.2012.09.010>
- [4]. Chai, Q., Jiao, Y., & Yu, X. (2017). Hydrogels for Biomedical Applications: Their Characteristics and the Mechanisms behind Them. *Gels*, 3(1), 6. <https://doi.org/10.3390/gels301000>
- [5]. Benamer, S., Mahlous, M., Boukrif, A., Mansouri, B., & Youcef, S. L. (2006). Synthesis and characterisation of hydrogels based on poly(vinyl pyrrolidone). *Nuclear Instruments and Methods in Physics Research, Section B: Beam Interactions with Materials and Atoms*, 248(2), 284–290. <https://doi.org/10.1016/j.nimb.2006.04.072>
- [6]. Ahmed, E. M. (2015). Hydrogel: Preparation, characterization, and applications: A review. *Journal of Advanced Research*. Elsevier B.V. <https://doi.org/10.1016/j.jare.2013.07.006>
- [7]. RATNER, B. D., & HOFFMAN, A. S. (1976). Synthetic Hydrogels for Biomedical Applications (pp. 1–36). <https://doi.org/10.1021/bk-1976-0031.ch001>
- [8]. Benamer, S., Mahlous, M., Boukrif, A., Mansouri, B., & Youcef, S. L. (2006). Synthesis and characterisation of hydrogels based on poly(vinyl pyrrolidone). *Nuclear Instruments and Methods in Physics Research, Section B: Beam Interactions with Materials and Atoms*, 248(2), 284–290. <https://doi.org/10.1016/j.nimb.2006.04.072>
- [9]. Drury, J. L., & Mooney, D. J. (2003). Hydrogels for tissue engineering: Scaffold design variables and applications. *Biomaterials*. Elsevier BV. [https://doi.org/10.1016/S0142-9612\(03\)00340-5](https://doi.org/10.1016/S0142-9612(03)00340-5)
- [10]. Hu, W., Wang, Z., Xiao, Y., Zhang, S., & Wang, J. (2019, March 1). Advances in crosslinking strategies of biomedical hydrogels. *Biomaterials Science*. Royal Society of Chemistry. <https://doi.org/10.1039/c8bm01246f>
- [11]. Lin, C. C., & Anseth, K. S. (2009, March). PEG hydrogels for the controlled release of biomolecules in regenerative medicine. *Pharmaceutical Research*. <https://doi.org/10.1007/s11095-008-9801-2>
- [12]. Guo, R., Su, Q., Zhang, J., Dong, A., Lin, C., & Zhang, J. (2017). Facile Access to Multisensitive and Self-Healing Hydrogels with Reversible and Dynamic Boronic Ester and

Disulfide Linkages. *Biomacromolecules*, 18(4), 1356–1364.
<https://doi.org/10.1021/acs.biomac.7b00089>

[13]. Vacanti, J. P., & Vacanti, C. A. (2013). The History and Scope of Tissue Engineering. In *Principles of Tissue Engineering: Fourth Edition* (pp. 3–8). Elsevier Inc.
<https://doi.org/10.1016/B978-0-12-398358-9.00001-X>

[14]. El-Sherbiny, I. M., & Yacoub, M. H. (2013). Hydrogel scaffolds for tissue engineering: Progress and challenges. *Global Cardiology Science and Practice*, 2013(3), 38.
<https://doi.org/10.5339/gcsp.2013.38>

[15]. Huang, T., Xu, H., Jiao, K., Zhu, L., Brown, H. R., & Wang, H. (2007). A novel hydrogel with high mechanical strength: A macromolecular microsphere composite hydrogel. *Advanced Materials*, 19(12), 1622–1626. <https://doi.org/10.1002/adma.200602533>

[16]. Wang, Q., Hou, R., Cheng, Y., & Fu, J. (2012). Super-tough double-network hydrogels reinforced by covalently compositing with silica-nanoparticles. *Soft Matter*, 8(22), 6048–6056. <https://doi.org/10.1039/c2sm07233e>

[17]. Zhang, Y. S., & Khademhosseini, A. (2017). Advances in engineering hydrogels. *Science*, 356(6337). <https://doi.org/10.1126/science.aaf3627>

[18]. Yu, L., & Ding, J. (2008). Injectable hydrogels as unique biomedical materials. *Chemical Society Reviews*, 37(8), 1473–1481. <https://doi.org/10.1039/b713009k>

[19]. Baldwin, A. D., & Kiick, K. L. (2013). Reversible maleimide-thiol adducts yield glutathione-sensitive poly(ethylene glycol)-heparin hydrogels. *Polymer Chemistry*, 4(1), 133–143. <https://doi.org/10.1039/c2py20576a>

[20]. Li, J., & Mooney, D. J. (2016, October 18). Designing hydrogels for controlled drug delivery. *Nature Reviews Materials*. Nature Publishing Group.
<https://doi.org/10.1038/natrevmats.2016.71>

[21]. Yang, W. J., Tao, X., Zhao, T., Weng, L., Kang, E. T., & Wang, L. (2015). Antifouling and antibacterial hydrogel coatings with self-healing properties based on a dynamic disulfide exchange reaction. *Polymer Chemistry*, 6(39), 7027–7035.
<https://doi.org/10.1039/c5py00936g>

[22]. Bastings, M. M. C., Koudstaal, S., Kieltyka, R. E., Nakano, Y., Pape, A. C. H., Feyen, D. A. M., ... Dankers, P. Y. W. (2014). A fast pH-switchable and self-healing supramolecular hydrogel carrier for guided, local catheter injection in the infarcted myocardium. *Advanced Healthcare Materials*, 3(1), 70–78.
<https://doi.org/10.1002/adhm.201300076>

[23]. Song, F., Li, X., Wang, Q., Liao, L., & Zhang, C. (2015, January 1). Nanocomposite

- hydrogels and their applications in drug delivery and tissue engineering. *Journal of Biomedical Nanotechnology*. American Scientific Publishers. <https://doi.org/10.1166/jbn.2015.1962>
- [24]. Injumba, W., Ritprajak, P., & Insin, N. (2017). Size-dependent cytotoxicity and inflammatory responses of PEGylated silica-iron oxide nanocomposite size series. *Journal of Magnetism and Magnetic Materials*, 427, 60–66. <https://doi.org/10.1016/j.jmmm.2016.11.015>
- [25]. Gaharwar, A. K., Rivera, C. P., Wu, C.-J., & Schmidt, G. (2011). Transparent, elastomeric and tough hydrogels from poly(ethylene glycol) and silicate nanoparticles. *Acta Biomaterialia*, 7(12), 4139–4148. <https://doi.org/10.1016/j.actbio.2011.07.023>
- [26]. Götz, W., Tobiasch, E., Witzleben, S., & Schulze, M. (2019). Effects of silicon compounds on biomineralization, osteogenesis, and hard tissue formation. *Pharmaceutics*, 11(3), 1–27. <https://doi.org/10.3390/pharmaceutics11030117>
- [27]. Bagheri, E., Ansari, L., Abnous, K., Taghdisi, S. M., Charbgoor, F., Ramezani, M., & Alibolandi, M. (2018). Silica based hybrid materials for drug delivery and bioimaging. *Journal of Controlled Release : Official Journal of the Controlled Release Society*, 277, 57–76. <https://doi.org/10.1016/j.jconrel.2018.03.014>
- [28]. Alothman, Z. A. (2012). A review: Fundamental aspects of silicate mesoporous materials. *Materials*. <https://doi.org/10.3390/ma5122874>
- [29]. Wang, N., Ma, M., Luo, Y., Liu, T., Zhou, P., Qi, S., ... Chen, H. (2018). Mesoporous Silica Nanoparticles-Reinforced Hydrogel Scaffold together with Pinacidil Loading to Improve Stem Cell Adhesion. *ChemNanoMat*, 4(7), 631–641. <https://doi.org/10.1002/cnma.201800026>
- [30]. Rosenholm, J. M., Zhang, J., Linden, M., & Sahlgren, C. (2016). Mesoporous silica nanoparticles in tissue engineering--a perspective. *Nanomedicine (London, England)*, 11(4), 391–402. <https://doi.org/10.2217/nmm.15.212>
- [31]. Jafari, S., Derakhshankhah, H., Alaei, L., Fattahi, A., Varnamkhasti, B. S., & Saboury, A. A. (2019, January 1). Mesoporous silica nanoparticles for therapeutic/diagnostic applications. *Biomedicine and Pharmacotherapy*. Elsevier Masson SAS. <https://doi.org/10.1016/j.biopha.2018.10.167>
- [32]. Zhang, Z., Wang, S., Waterhouse, G. I. N., Zhang, Q., & Li, L. (2019). Poly(N -isopropylacrylamide)/mesoporous silica thermosensitive composite hydrogels for drug loading and release. *Journal of Applied Polymer Science*, 48391. <https://doi.org/10.1002/app.48391>

- [33]. Wang, N., Ma, M., Luo, Y., Liu, T., Zhou, P., Qi, S., ... Chen, H. (2018). Mesoporous Silica Nanoparticles-Reinforced Hydrogel Scaffold together with Pinacidil Loading to Improve Stem Cell Adhesion. *ChemNanoMat*, 4(7), 631–641. <https://doi.org/10.1002/cnma.201800026>
- [34]. Du, J., Wang, D., Xu, S., Wang, J., Liu, Y., & Huang, J. (2017). Stretchable dual nanocomposite hydrogels strengthened by physical interaction between inorganic hybrid crosslinker and polymers. *Applied Clay Science*, 150, 71–80. <https://doi.org/10.1016/j.clay.2017.09.008>
- [35]. Xu, B., Wang, L., Liu, Y., Zhu, H., & Wang, Q. (2018). Preparation of high strength and transparent nanocomposite hydrogels using alumina nanoparticles as cross-linking agents. *Materials Letters*, 228, 104–107. <https://doi.org/10.1016/j.matlet.2018.05.135>
- [36]. Valentina Cauda, Axel Schlossbauer, Johann Kecht, Andreas Zu'rner, and T. B. (2009). Multiple Core-Shell Functionalized Colloidal Mesoporous Silica Nanoparticles. *J. AM. CHEM. SOC.*, 131, 11361–11370
- [37]. Mansfield, E. D. H., Pandya, Y., Mun, E. A., Rogers, S. E., Abutbul-Ionita, I., Danino, D., ... Khutoryanskiy, V. V. (2018). Structure and characterisation of hydroxyethylcellulose-silica nanoparticles. *RSC Advances*, 8(12), 6471–6478. <https://doi.org/10.1039/c7ra08716k>
- [38]. Mannervik, B. (1999). Measurement of Glutathione Reductase Activity. *Current Protocols in Toxicology*, 00(1), 7.2.1-7.2.4. <https://doi.org/10.1002/0471140856.tx0702s00>
- [39]. Wu, G., Fang, Y.-Z., Yang, S., Lupton, J. R., & Turner, N. D. (2004). Glutathione Metabolism and Its Implications for Health. *The Journal of Nutrition*, 134(3), 489–492. <https://doi.org/10.1093/jn/134.3.489>
- [40]. [https://chem.libretexts.org/Under_Construction/Purgatory/Book%3A_Organic_Chemistry_with_a_Biological_Emphasis_\(Soderberg\)/16%3A_Oxidation_and_reduction_reactions/16.12%3A_Redox_reactions_involving_thiols_and_disulfides?fbclid=IwAR0kF61eb4r7LPk80TUVvzAtOBmlF4NW1a2wZc3pNdJgDMii3vk88wPJbVU](https://chem.libretexts.org/Under_Construction/Purgatory/Book%3A_Organic_Chemistry_with_a_Biological_Emphasis_(Soderberg)/16%3A_Oxidation_and_reduction_reactions/16.12%3A_Redox_reactions_involving_thiols_and_disulfides?fbclid=IwAR0kF61eb4r7LPk80TUVvzAtOBmlF4NW1a2wZc3pNdJgDMii3vk88wPJbVU), on 25th of August 2019
- [41]. Gehrke, S. H., Fisher, J. P., Palasis, M., & Lund, M. E. (1997). Factors determining hydrogel permeability. *Annals of the New York Academy of Sciences*, 831, 179–207. <https://doi.org/10.1111/j.1749-6632.1997.tb52194.x>

Supplementary Information

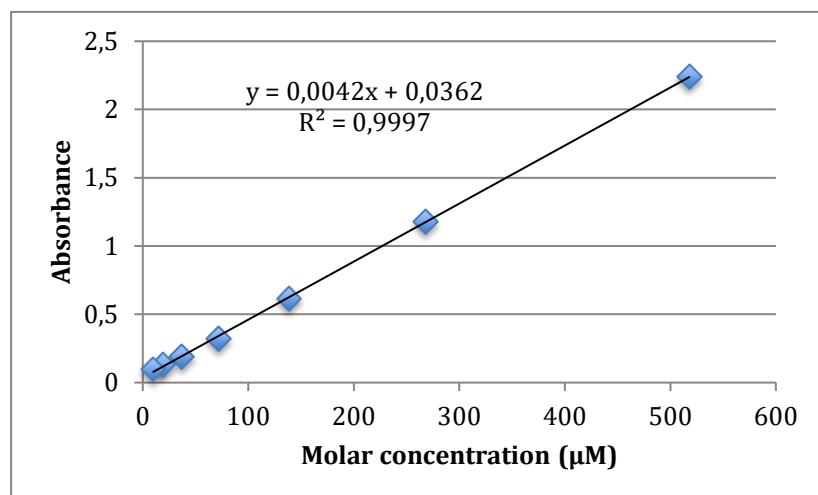


Figure S1 -Calibration curve of Cystein-HCL

By linear regression, the curve obtain had a R^2 of 0,99971 and the equation was $y = 0.0042x+0.0362$



Figure S2 - Different solutions of DTNB

From right to left, there is the buffer with DTNB, PBS solution with a old DTNB flask and PBS with a fresh DTNB flask.

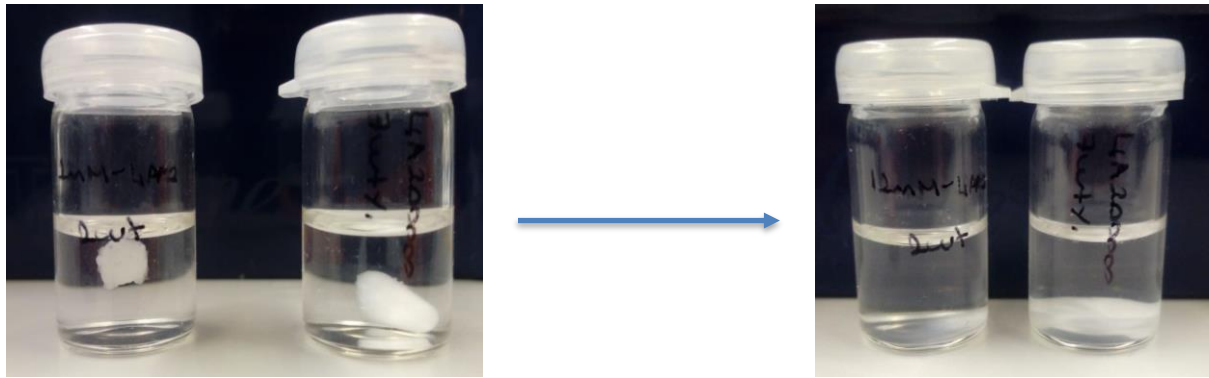


Figure S3 - Hydrogel degradation with 5mM
After 24h at room temperature, the hydrogel degraded in a 5mM solution of GSH

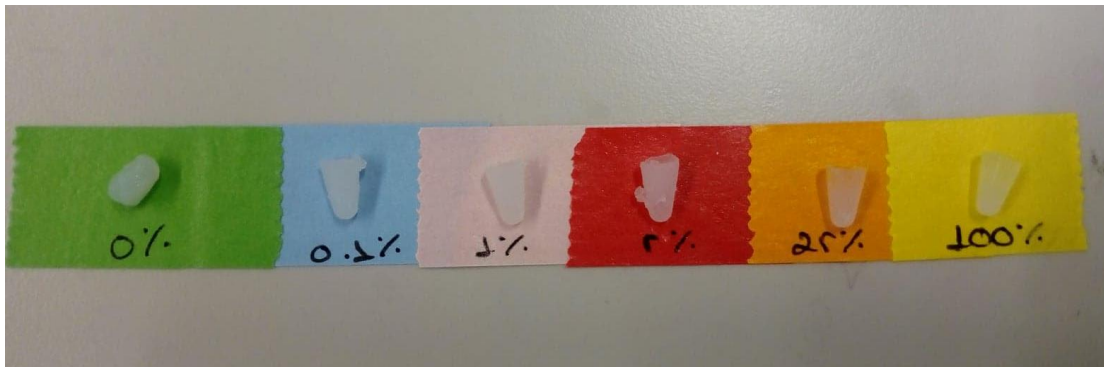


Figure S4- Hydrogel formation with different functionalization of MSN
Hydrogels were formed with MSN as crosslinker but with different functionalization the the surface. Each percentage corresponde to the functionalization of MSN, being 100% as described in synthesis